

# Hydrocarbon Potentials of Baze Field, Onshore Niger Delta, Nigeria: Petrophysical Analysis and Structural Mapping

M. K. Salami<sup>1,\*</sup>, A. Amuni<sup>1</sup>, T. Adewumi<sup>2</sup>, J. Asare<sup>1</sup>, O. K. Oyewole<sup>1,3</sup>

<sup>1</sup>Department of Physics, Baze University, Abuja, Federal Capital Territory, Nigeria

<sup>2</sup>Department of Physics, Federal University, P.M.B. 146, Lafia, Nassarawa State, Nigeria

<sup>3</sup>Department of Mechanical Engineering, Worcester Polytechnic Institute, 100 Institute Road, Worcester, MA 01609, USA

\*Corresponding author: [salami.muyideen@bazeuniversity.edu.ng](mailto:salami.muyideen@bazeuniversity.edu.ng), [muyideensalami@gmail.com](mailto:muyideensalami@gmail.com)

**Abstract** This paper presents the results of the reservoir characterization of Baze field, Niger Delta, Nigeria, using seismic and well log data. The area of the field is bounded with longitudes 3.00°E and 7.00°E, and latitudes 4.00°N and 8.00°N. Analysis of the structural maps of five horizons showed the structural geometry of the subsurface and the presence of possible trapping mechanism, which control the accumulation of hydrocarbons in the Baze field. Interpretations of faults that described the structural setting of the field showed two major faults trends from East to West while dipping southward with other minor (synthetic and antithetic) faults. Petrophysical parameters are estimated to determine reservoir properties, while the hydrocarbon volumetric reserves are calculated with total oil and gas recoverable estimates of 6.115 MMBbls and 8.456 Bscf respectively. From the reservoir characterizations done in this research work, the Baze field located onshore of the Niger Delta has been identified as suitable for hydrocarbon production.

**Keywords:** accumulation, characterization, hydrocarbon, petrophysical, seismic data and onshore

**Cite This Article:** M. K. Salami, A. Amuni, T. Adewumi, J. Asare, and O. K. Oyewole, "Hydrocarbon Potentials of Baze Field, Onshore Niger Delta, Nigeria: Petrophysical Analysis and Structural Mapping." *Journal of Geosciences and Geomatics*, vol. 6, no. 2 (2018): 55-64. doi: 10.12691/jgg-6-2-3.

## 1. Introduction

The demand for energy in the world has increased over the past five (5) decades [1]. This has led to greater challenge for optimization and continuous efforts that can lead to a constant supply of the energy to the people. In Nigeria, oil and gas is a very important source of revenue for national development. Therefore, there is a need for both Government and research institutions to ensure that this non-renewable resource is adequately and optimally tapped.

The production of oil and gas in Nigeria today is in Niger Delta province, which has commercial accumulation of oil and gas. The production is from accumulation in the pore spaces of reservoir rocks, usually sandstone [1]. The reservoir in the Niger Delta is characterized by alternation of sandstone and shale units ranging in thickness from 100 ft to 1500 ft [2,3]. The sand in this formation is mainly hydrocarbon reservoir with shale providing lateral and vertical seal.

Reservoir characterization and subsurface geological mapping are perhaps one of the most important techniques that are used in the exploration of undiscovered hydrocarbons and development of proven hydrocarbon reserves. As a field is developed from its initial discovery, a large volume of well, seismic, and production data are obtained. Integration of these data sets improves the accuracy of the

interpretation of the subsurface. 3D seismic interpretation often requires extrapolating well data far from the area of interest, crossing faults, sequence boundaries, and other discontinuities [4]. Well data gives a variety of information regarding the lithology (such as mineralogy, porosity, and also the morphology of the pore spaces), the fluid content and detailed depth constraints on geologic horizons [5].

In an effort to contribute to the improvement of oil and gas production in the world, we explore the characterization of Baze field in Niger Delta of Nigeria through imaging of the subsurface structures by mapping faults, identifying the lithology and map reservoirs in the field and determining the reservoir properties and volume of hydrocarbon within reservoirs of the Baze field.

### 1.1. Location and Geology of the Study Area

The study area (Baze field) is located in the onshore area of the Niger Delta, Nigeria which lies between longitudes 3.00°E and 7.00°E, and latitudes 4.00°N and 8.00°N (Figure 1). The Niger Delta is situated in the Gulf of Guinea, West Africa. It represents the southern margin of a triple junction rift system that triggered the separation of the African continent from the South American continent during the Jurassic through the Early Cretaceous. Rifting started around late Jurassic and continued to the middle Cretaceous [6]. During the Late Cretaceous, rifting reduced. Figures 2A and 2B depict the gross paleogeography

of the Niger Delta and the relative positions of the African and South American plates from the period of rifting. At

the end of rifting, gravity tectonism occurred as the main process of deformation [6].

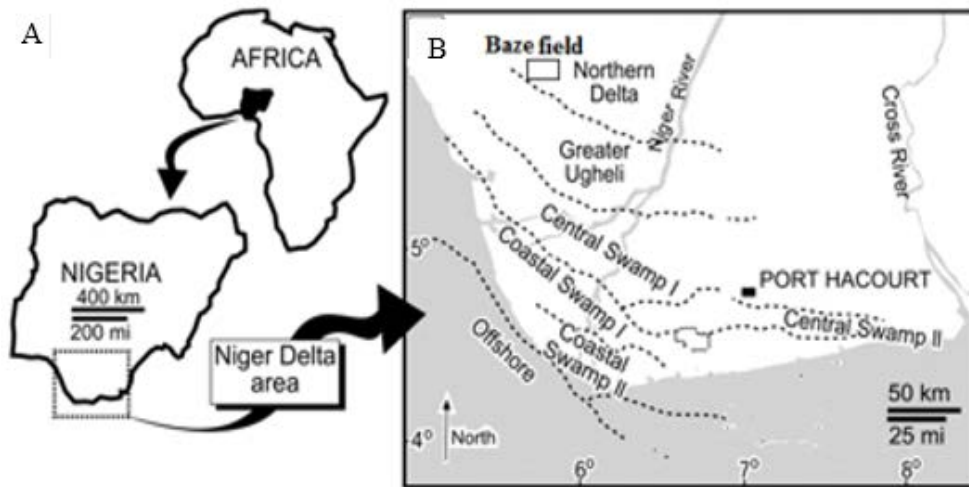


Figure 1. (A) Position of Nigeria in Africa and the Niger Delta Basin; (B) The Baze field location map [6]

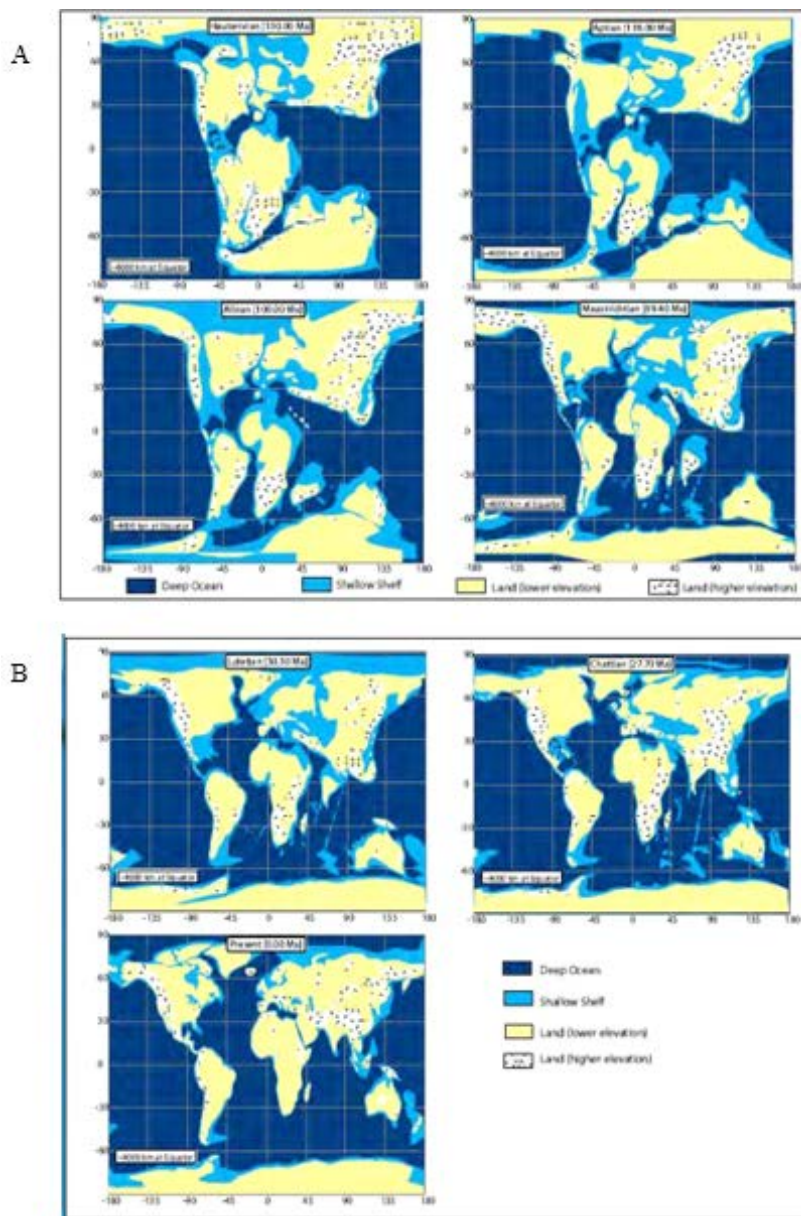
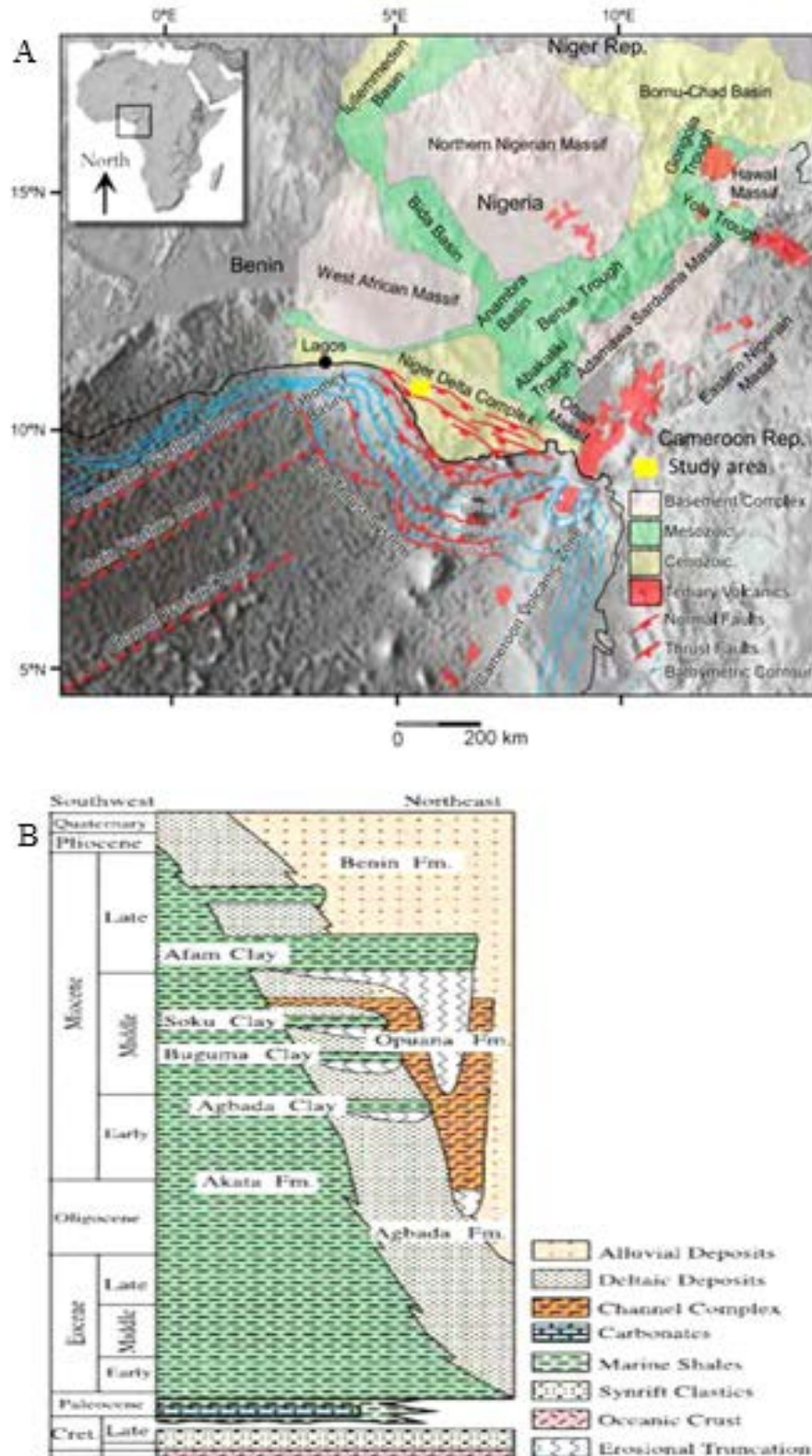


Figure 2. Paleogeography revealing the opening of the South Atlantic, and development of the region around the Niger Delta (A) Cenozoic paleogeography (B) Cretaceous paleogeography (Tuttle et al., 1999)

Internal deformation was induced by the mobility of shale. This occurred as a result of the response to the two major processes as explained by [7]. The first process was the formation of shale diapirs from the loading of Akata formation which was poorly compacted, over-pressured, pro-delta and delta-slope clays, by the more densely delta front sands which is the Agbada formation. The second process involved the instability of

slope [8] which occurred as a result of lack of lateral, basin ward, and support for the Akata formation. There was completion of gravity tectonics for any depo-belts in the Niger Delta before Benin formation was deposited. These are shown in complex structures such as roll-over anticlines, shale diapirs, collapsed growth faults, back-to-back features and steeply dipping closely spaced flank faults [8].



**Figure 3.** (A) The bounding geologic features of the Niger delta depicting the northern sources of fluvial supply [1]. (B) Stratigraphic column depicting the three formations of the Niger Delta [2]



## 1.2. Stratigraphy Settings of the Study Area

The stratigraphy settings of the study area shows that the River Niger is the main supplier of sediments to the Niger delta [9]. River Benue (which is the second prominent fairway of sediment supply to the Niger delta) merges with River Niger in the confluence town of Lokoja, Nigeria. River Niger subsequently branches into a network of tributaries that deposit their fluvial load into the Niger delta. Sediment supply to the Niger delta is sourced from the Northern Nigerian massif, the West African massif, Adamawa Massif, Oban massif, Benue trough, Bida basin, Anambra basin, and Abakaliki trough [9] (Figure 3A). The Niger delta lithology is predominantly siliciclastic, and the direction of current at discharge to the Niger delta is approximately north-south (N-S). The Niger delta is believed to have been prograding into the Atlantic Ocean for the last 35 Ma. Each formation records a different part of a linked non-marine to delta to offshore depositional system.

Reference [3] sub-divided the Niger delta into three litho-stratigraphic units, ranging in age from Paleocene to Recent. They include the Akata, Agbada and Benin formations (Figure 3B). These formations are coeval. The Akata formation is marine in origin and it is made up of thick shale sequences. The Akata formation is situated at the base of the Niger Delta and consists of pro-delta, hemipelagic, and pelagic shales that were deposited in marine environments. The formation is late Paleocene to early Pliocene in age. The Akata formation is characterized by high plasticity and overpressure, especially at depth. All major faults and counter-regional faults merge into a plane (or detachment surface) in the lower part of the Akata formation. Though little of the Akata formation has been drilled with the availability of only top structure map of the formation, estimations show that the formation is about 23,000ft, (7,000 m) in thickness [2,10]. The Agbada formation consists of a paralic sequence of interbedded sands and shales [2,10] The sandstones were deposited in prograding transitional or coastal environments comprised the fluvio-deltaic and barrier islands of the delta front, lagoon, brackish-water bays, beaches, and the shore face. Shales are pro-deltaic to hemipelagic in origin. The Agbada formation is Eocene to Pleistocene in age and about 3,700 m thick. The Benin formation consists of continental sandstones that were deposited in a delta plain as point bars by meandering streams or as channel fills with natural levees [2]. The massive fresh-water bearing Benin formation occurs widely across the Niger delta, with thicknesses ranging between 300 and 3,000 m. The Benin formation does not play any important role in the evolution of the Niger delta petroleum system, except serving as overburden.

## 2. Theory

In this section, some of the theories needed for estimation of petrophysical parameters are elucidated. These include: shale volume, porosity and water saturation.

### 2.1. Shale Volume

Shale volume is the amount of shale present in a porous formation. Shale volume ( $V_{sh}$ ) can be calculated using

gamma-ray logs by applying 'Larionov tertiary rock' method [11] as shown in equation 1 and 2:

$$GR_{index} = \frac{GR - GR_{matrix}}{GR_{shale} - GR_{matrix}}. \quad (1)$$

Larionov tertiary rock method is given by equation 2:

$$V_{sh} = 0.083 \times \left( 2^{(3.7 \times GR_{index})} - 1 \right) \quad (2)$$

Where GR is the gamma-ray (GR) log reading in the zone of interest;  $GR_{matrix}$  is the GR log reading in 100% matrix rock;  $GR_{shale}$  is the GR log reading in 100% shale;  $GR_{index}$  is the gamma-ray index;  $V_{sh}$  is the volume of shale.

### 2.2. Porosity

Porosity is a measure of the amount of void spaces present in a rock or formation. Porosity ( $\phi$ ) can be estimated from density log using equation 3 [12].

$$\phi_{density} = \frac{\rho_{ma} - \rho_{bulk}}{\rho_{ma} - \rho_{fluid}} \quad (3)$$

Where  $\phi_{density}$  is the density porosity,  $\rho_{ma}$  is the matrix density,  $\rho_{bulk}$  is the bulk density and  $\rho_{fluid}$  is the fluid density

### 2.3. Water Saturation

Water saturation is the ratio of the volume of water to the volume of pore space present in a rock or formation. Water saturation for the field was calculated using the Archie's water saturation equation in equation 4;

$$S_w = \left[ (a/\phi^m) \times (R_w/R_t)^{1/n} \right]. \quad (4)$$

Hydrocarbon saturation was then calculated using equation (5) [12].

$$S_h = 1 - S_w \quad (5)$$

Where  $S_w$  is the water saturation,  $\phi$  is the porosity,  $R_w$  is the formation water resistivity and  $R_t$  is the observed bulk resistivity,  $a$  is a constant,  $m$  is the cementation factor and  $n$  is the saturation exponent.

### 2.4. Estimation of Reserves

In an effort to estimate reserves, deterministic method can be used to compute the hydrocarbon reserves in the study area. The GRV can be computed from the structural depth maps, which can be interpreted from seismic data. With the petrophysical variables (that include: porosity, water saturation and the net-to-gross), the volume of oil reserves in any field can be calculated using:

$$STOIP = \frac{7758(N/G)V_B\phi(1-S_{iw})}{B_0} \quad (6)$$

Where STOIP is the Stock Tank Oil Initially In Place, N/G is the Net/Gross ratio,  $V_B$  is the bulk volume in Acre - ft,  $\phi$  is the average porosity,  $S_{iw}$  is the irreducible water saturation and  $B_0$  is the oil formation volume factor.

The volumetric equation for gas reserves is given by (Asquith, 2004):

$$GIIP = \frac{43560(N/G)V_B\phi(1-S_{iw})}{B_g} \quad (7)$$

Where, GIIP is the Gas Initially in Place (in SCF), N/G = Net/Gross ratio,  $V_B$  is the bulk volume in Acre – ft,  $\phi$  is the average porosity,  $S_{iw}$  = irreducible water saturation and  $B_g$  is the Gas formation volume factor.

### 3. Materials and Methods

3D seismic data, well deviation data, checkshot data and well logs were collected from Oriental Energy Resources Limited. These were loaded into Petrel software and carefully examined to determine the extent of the wells and logs present. The base map of the wells was then generated from petrel, while the well correlation was done using both the gamma ray logs and the resistivity logs. The gamma ray log, neutron density logs and resistivity logs were used to identify the contacts of the hydrocarbon bearing reservoirs.

The processed seismic data were saved in SEG-Y format (Society of Exploration Geophysics Format-Y) before being loaded into Petrel software. The seismic volume has an inline from 5800 to 6200 and a crossline from 1480 to 1700. The four well logs were saved in LAS format (Log ASCII Standard Format).

In an effort to characterize the Baze field by estimating the volumetric oil and gas reserves, the shale volume ( $V_{sh}$ ) was calculated using equations 1 and 2, while the porosity

was computed using the density log from equation 3. The water saturation of the field was calculated using equations 4 and 5. The calculated petrophysical parameters were then used to estimate the volumetric oil and gas reserves using equations 6 and 7.

## 4. Result and Discussion

### 4.1. Presentation of Well Correlations and Properties

The plotted wells are presented in Figure 4. Hydrocarbon-bearing sands were identified from the deep resistivity and gamma ray logs. Six sand units were identified across the wells namely; reservoir A, B, C, D, E and F. The sands were laterally correlated across the four wells strictly on the basis of litho-stratigraphic properties (sand quality and log motif). The gamma ray signature of the identified sand units and the base map was used to determine the direction of deposition in the field. The direction of deposition in the field was discovered to be from Northwest (NW) to South-East (SE).

Petrophysical evaluation was carried out in the study area and the fluids present in the reservoirs (A, B, C, D, E and F) were identified across the four wells in Baze field. The fluids in the field were controlled by the compartmentalization caused by complex faulting. Two major faults were penetrated by the wells in the field, and these wells encountered the hydrocarbon-bearing sands at different depths as described below in Table 1 – Table 4.

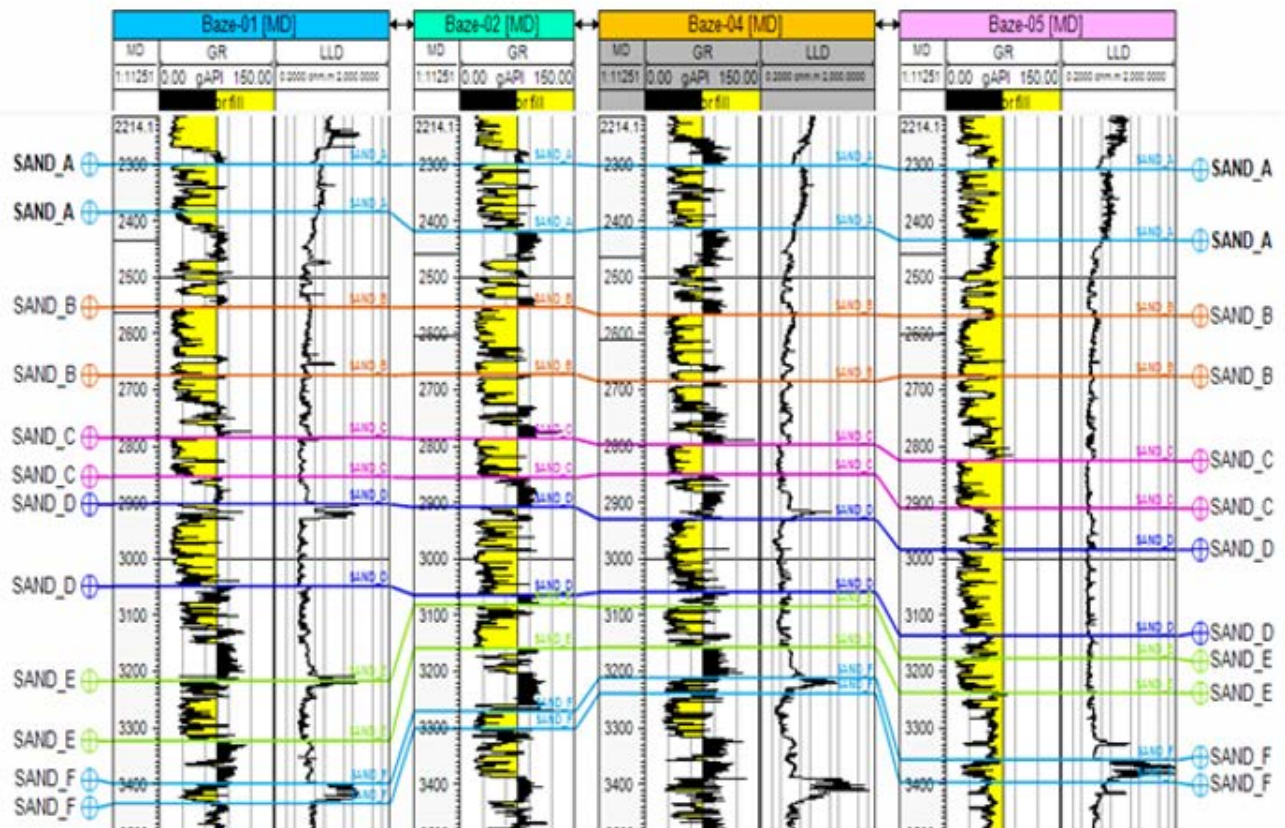


Figure 4. Well correlation of MD Baze field Onshore, Niger Delta

Table 1. Fluid contact in Baze-01 well

Reservoir	Baze-01		Hydrocarbon Thickness (m)	Fluid Contact		Contact Type
	Top (m)	Base (m)		Top (m)	Base (m)	
A	2442.70	2462.18	6.45	2442.70	2449.15	OWC
B	2622.99	2643.50	4.5	2622.99	2627.49	OWC
C	2752.12	2794.15	7.11	2752.12	2759.23	OWC
D	2910.61	2910.61	28.26	2871.02	2899.28	OWC
E	3175.19	3210.62	20.08	3175.19	3195.27	OWC
F	3366.41	3399.90	29.89	3366.41	2296.30	OWC

Table 2. Fluid contact in Baze-02 well

Reservoir	Baze-02		Hydrocarbon Thickness (m)	Fluid Contact		Contact Type
	Top (m)	Base (m)		Top (m)	Base (m)	
A	2442.42	2459.83	17.41	2442.42	2459.83	OWC
B	2618.98	2643.64	24.66	2618.98	2643.64	OWC
C	2754.71	2788.90	34.19	2754.71	2788.90	OWC
D	2877.35	2929.54	52.19	2877.35	2929.54	OWC
E	3226.31	3283.15	56.84	3226.31	3283.15	OWC
F	3396.10	3422.95	26.85	3396.10	3422.95	OWC

Table 3. Fluid contact in Baze-04 well

Reservoir	Baze-04		Hydrocarbon Thickness (m)	Fluid Contact		Contact Type
	Top (m)	Base (m)		Top (m)	Base (m)	
A	2453.14	2475.32	22.18	2453.14	2475.32	OWC
B	2639.23	2657.05	17.82	2639.23	2657.05	OWC
C	2769.16	2824.49	15.53	2769.16	2824.49	OWC
D	2884.39	2913.76	18.03	2884.39	2902.42	OWC
E	3181.55	3208.39	8.75	3181.55	3190.30	GOC
E	3190.30	3201.23	8.27	3190.30	3198.58	OWC
F	3358.75	3409.76	43.13	3358.75	3401.88	OWC

Table 4. Fluid contact in Baze-05 well

Reservoir	Baze-05		Hydrocarbon Thickness (m)	Fluid Contact		Contact Type
	Top (m)	Base (m)		Top (m)	Base (m)	
A	2640.73	2479.38	38.65	2640.73	2679.38	OWC
B	2653.24	2676.25	23.01	2653.24	2676.25	OWC
C	2794.78	2879.12	15.66	2794.78	2779.12	OWC
D	2924.89	2986.31	21.42	2964.89	2986.31	OWC
E	3196.72	3253.83	17.11	3296.72	3313.83	OWC
F	3323.96	3357.06	33.10	3323.96	3357.06	OWC

In the reservoirs A, B, and C at different depths of 2449.15 m, 2627.49 m and 2759.23 m respectively, Baze-01 well encountered an oil–water contact (OWC). However, Baze-04 well in the same fault compartment also encountered the reservoir as OWC. Both Baze-02 and Baze-05 in the downthrown fault compartment encountered the reservoir as OWC.

Likewise in reservoir D at the depth of 2899.28, Baze-01 well encountered an OWC in the upthrown fault compartment, while Baze-04 well in the same fault compartment encountered the reservoir as an oil–water–contact (OWC) at a depth of 2902.42 m. Both Baze-02 and Baze-05 in the downthrown fault compartment encountered the reservoir as OWC.

In reservoir E, at the depth of 3195.27 m, Baze-01 well encountered an OWC in the upthrown fault compartment, while Baze-04 well in the same fault compartment encountered an OWC at 3190.30 m and a gas–oil–contact (GOC) at 3198.58 m, respectively. However, Baze-05 in the same upthrown fault compartment encountered the reservoir as OWC, while Baze-02 well in the downthrown fault compartment encountered the reservoir as OWC.

Finally, in reservoir F at the depth of 3396.30 m, Baze-01 well encountered an OWC in the upthrown fault compartment, while Baze-04 well in the same fault compartment encountered the sand as an OWC at 3401.88 m; Baze-05 also in the same upthrown fault compartment encountered the Reservoir as an oil–water–contact OWC situation at a depth of 3357.06 m. Baze-02 well in the downthrown fault compartment encountered the reservoir as OWC.

The estimated averages reservoir properties in the field are presented in Table 5 - Table 8. The average reservoir properties were calculated over the defined gross reservoir interval and net pay intervals.

From Table 5 – Table 8, it could be inferred that hydrocarbon thickness in Baze-01 ranges between 4.51 - 29.89 m with an average of 16.05 m. Reservoirs in Baze-02 show hydrocarbon thickness between 9.15 – 32.19 m with an average of 15.95 m. In Baze-04, reservoirs thicknesses are between 10.12 - 42.13 m. Likewise in Baze-05, reservoirs A-E thicknesses are between 18.65 - 57.11 m (Table 5 – Table 8). While the average porosity in Baze-01 ranges from 0.22 to 0.28, 0.22 to 0.25 in Baze-04, 0.22 to 0.27 in Baze-02 and 0.24 to 0.27 in Baze-05 respectively.



**Table 5. Average reservoir properties in Baze-01**

Reservoir	Top (m)	Base (m)	Gross Reservoir (m)	Net Pay (m)	NTG (fraction)	Average Porosity (fraction)	Average Sw (fraction)
A	2442.70	2462.18	19.48	5.76	0.30	0.24	0.25
B	2622.99	2643.50	20.51	3.48	0.17	0.28	0.33
C	2752.12	2794.15	42.03	5.76	0.14	0.27	0.31
D	2910.61	2910.61	39.58	18.33	0.46	0.23	0.24
E	3175.19	3210.62	35.43	11.21	0.32	0.23	0.22
F	3366.41	3399.90	33.49	21.36	0.64	0.22	0.21

**Table 6. Average reservoir properties in Baze-02**

Reservoir	Top (m)	Base (m)	Gross Reservoir (m)	Net Pay (m)	NTG (fraction)	Average Porosity (fraction)	Average Sw (fraction)
A	2442.42	2459.83	17.41	9.46	0.54	0.22	0.27
B	2618.98	2643.64	24.66	10.40	0.42	0.26	0.31
C	2754.71	2788.90	34.19	9.15	0.27	0.27	0.30
D	2877.35	2929.54	52.18	32.19	0.62	0.24	0.26
E	3226.31	3283.15	56.85	20.25	0.36	0.26	0.20
F	3396.10	3422.95	26.85	14.25	0.53	0.22	0.23

**Table 7. Average reservoir properties in Baze-04**

Reservoir	Top (m)	Base (m)	Gross Reservoir (m)	Net Pay (m)	NTG (fraction)	Average Porosity (fraction)	Average Sw (fraction)
A	2453.14	2475.32	22.17	10.12	0.46	0.20	0.25
B	2639.23	2657.05	17.82	6.52	0.37	0.25	0.31
C	2769.16	2824.49	55.33	20.00	0.36	0.27	0.28
D	2884.39	2913.76	29.36	0.91	0.03	0.25	0.26
E	3181.55	3208.39	26.84	10.30	0.38	0.23	0.28
F	3358.75	3409.76	51.01	18.03	0.35	0.22	0.24

**Table 8. Average reservoir properties in Baze-05**

Reservoir	Top (m)	Base (m)	Gross Reservoir (m)	Net Pay (m)	NTG (fraction)	Average Porosity (fraction)	Average Sw (fraction)
A	2640.73	2479.38	18.65	12.30	0.66	0.24	0.29
B	2653.24	2676.25	23.00	9.85	0.43	0.22	0.28
C	2794.78	2879.12	34.34	24.60	0.29	0.24	0.31
D	2924.89	2986.31	61.42	35.45	0.58	0.25	0.28
E	3196.72	3253.83	57.11	34.65	0.61	0.27	0.23
F	3323.96	3357.06	33.10	7.12	0.22	0.25	0.21

## 4.2. Seismic Interpretation

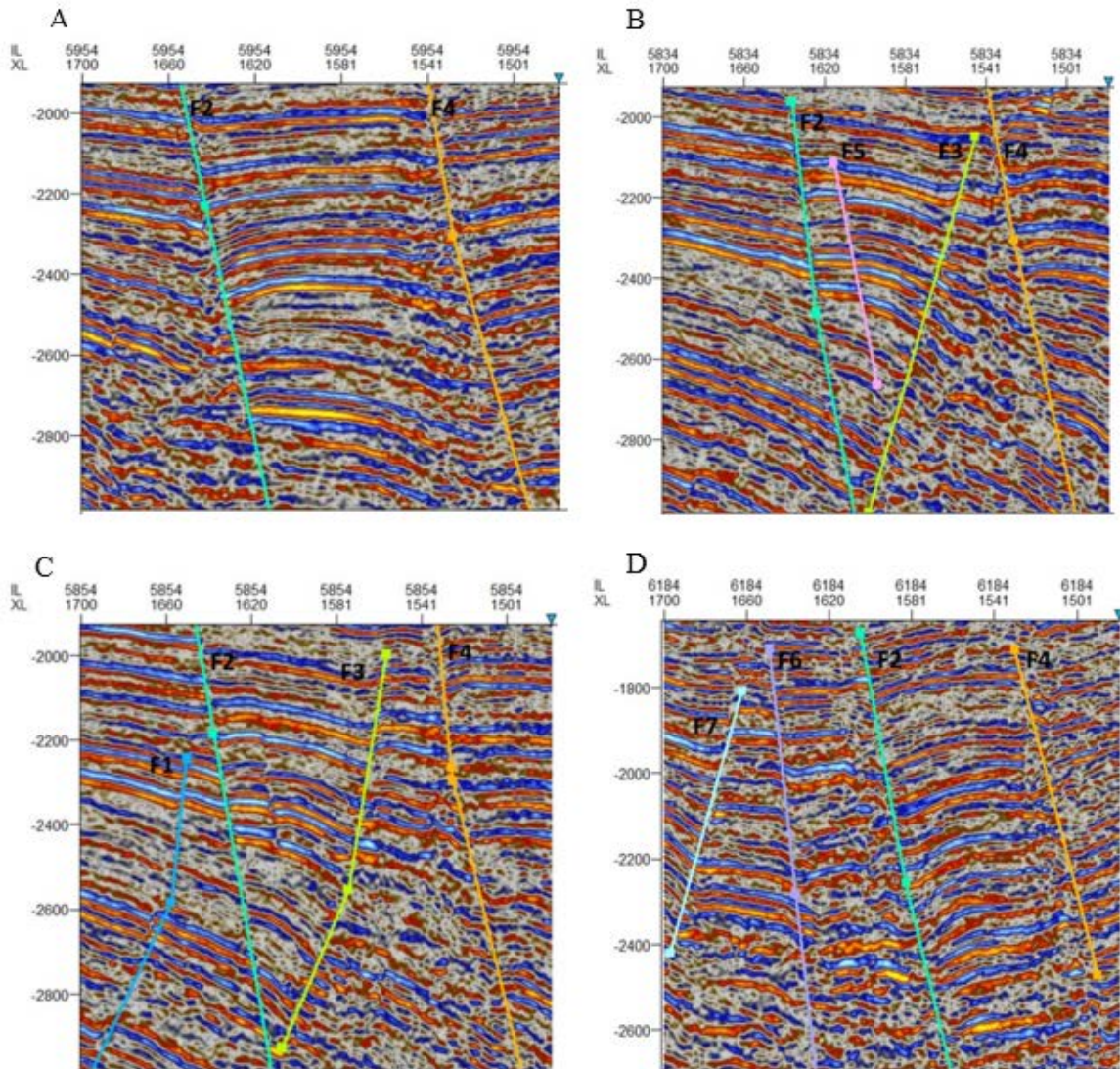
Figure 5A – Figure 5D reveal the kind of structures (faults) present in the field and are labelled F2 and F4 as seen on seismic sections. The major and minor faults observed across the seismic sections were mapped to delineate the hydrocarbon structural trapping mechanism of the field. The structure in Baze field is dominated by two major listric normal faults, trending East-West (E -W) and dipping towards the south which corresponds to gravity tectonics that occurred as a response to variable rates of subsidence and sediment supply.

Synthetic and antithetic minor faults of small scale radiate from anticline crests, which makes those observed structures to be more complicated. The antithetic faults include F1, F3 and F7 while synthetic faults include F5 and F6 (Figures 5B-5D). The presence of these complex structures such as collapsed growth faults, back-to-back features in Baze field suggested that there was completion of gravity tectonics before Benin formation was deposited [8]. The two major faults are believed to act as conduits for the migration of hydrocarbon from the Akata formation to the overlying Agbada formation. The throw of the major faults is between 30 – 90 m while those of minor faults are between 3 – 24 m.

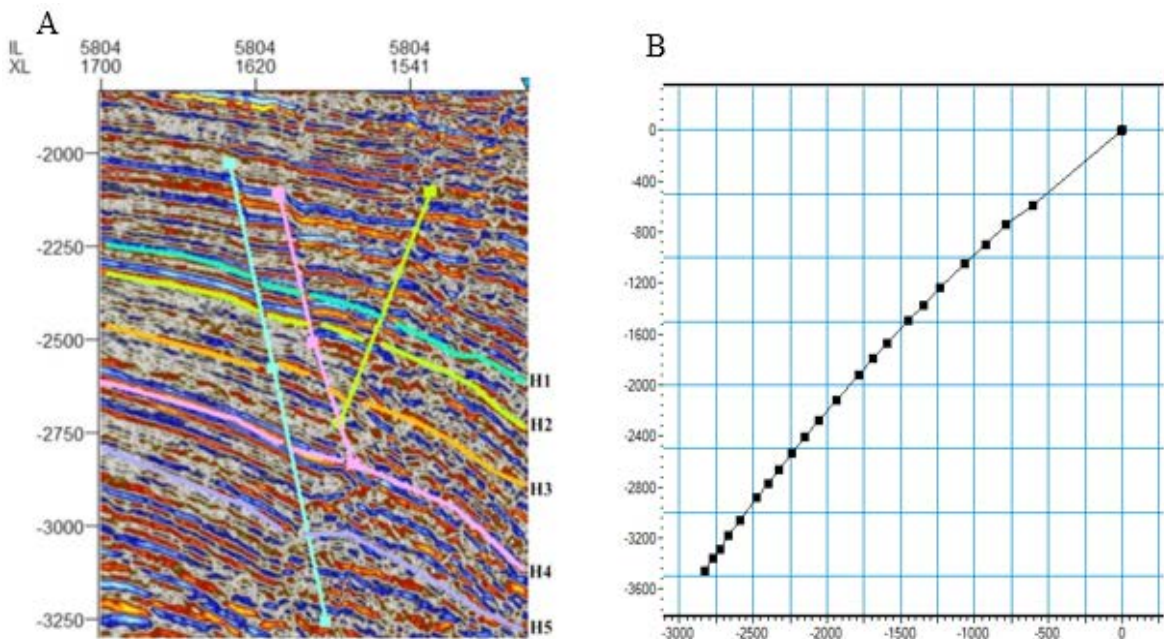
## 4.3. Horizon Interpretation

Figure 6A shows the five horizons (H1, H2, H3, H4 and H5) mapped, which corresponds to reservoir sands A, B, C, D, and E on the well logs. Horizons were picked on the incline and cross line sections across the seismic volume. The horizons were filled smoothed and contoured to form the time maps. The checkshot data was plotted on a graph of Two-way-time (TWT) against depth, the equation of the graph is the velocity model (Figure 6B). The velocity model was used to convert the time maps to depth structure maps. The five horizons picked namely: horizon A, horizon B, horizon C, horizon D and horizon E shows significant good structures.

Figures 7A – 7D shows that Horizons A, B, C, D and E has their deepest part at a depth of 2610 m, 3200 m, 3600 m and 3350 m respectively. While their shallowest part is at a depth of 1950 m, 1900 m, 2400 m, 2400 m and 2450 m respectively. The depth map shows the presence of faults assisted closures which are potential areas of hydrocarbon accumulations. The integration of the seismic data and the well logs shows the presence of a hydrocarbon bearing reservoir in which the wells Baze-05 and Baze-02 were drilled through. The hydrocarbon bearing reservoir falls between two faults which serves as a good hydrocarbon trapping mechanism.



**Figure 5.** (A) In-line 5954 showing mapped faults in Baze field (B) In-line 5834 showing mapped faults in Baze field (C) In-line 5854 showing mapped faults in Baze field (D) In-line 6184 showing mapped faults in Baze field



**Figure 6.** (A) Horizon mapping within Baze-field (B) Two-way-time (TWT) graph of the checkshot data



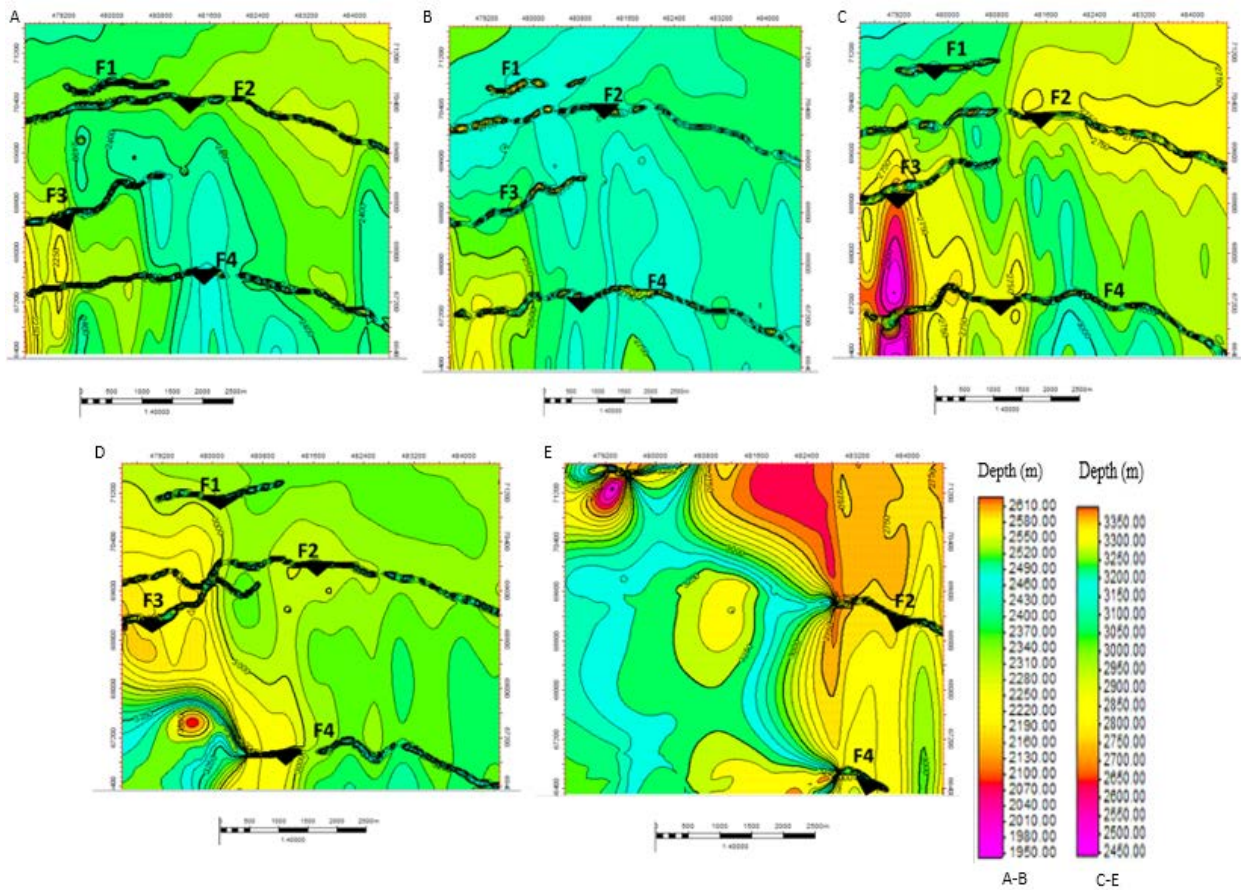


Figure 7. Depth structure maps in Baze Field for (A) reservoir A (B) reservoir B (C) reservoir C (D) reservoir D (E) reservoir E

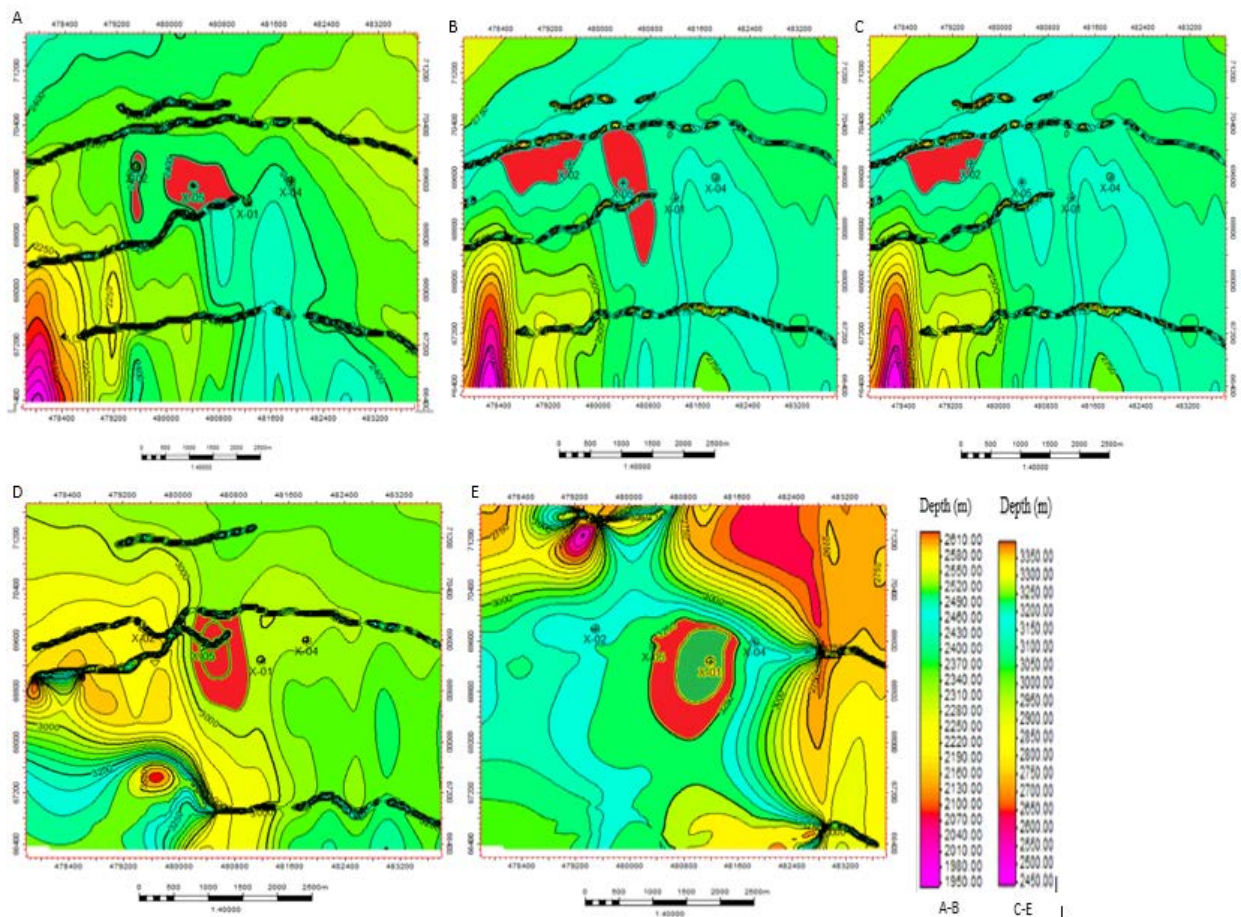


Figure 8. Depth structure maps showing hydrocarbon-bearing area for (A) reservoir A (B) reservoir B (C) reservoir C (D) reservoir D (E) reservoir E

Table 9. Porosity Description

Reservoir	Area (acre)	HC thickness (ft)	NTG	$\phi$	Sw	Bo	STOIIP (MMbbls)
A	502.123	19.09	0.30	0.24	0.25	1.135	10.95
B	736.932	11.48	0.17	0.28	0.33	1.135	8.35
C	550.215	19.09	0.14	0.27	0.31	1.135	6.23
D	300.035	31.75	0.25	0.24	0.30	1.135	4.56
E	200.543	35.51	0.35	0.23	0.25	1.135	4.944
F	600.234	51.15	0.40	0.23	0.22	1.135	5.35

Table 10. Volumetric Reservoir Data and Gas Reserves for Baze field

Reservoir	Area (acre)	HC thickness(ft)	NTG	$\phi$	Sw	Bg	GIIP (Bscf)
E	189.22	19.02	0.32	0.23	0.31	0.0017	14.094

Note: HC = hydrocarbon thickness, NTG = net-to-gross ratio,  $\phi$ = porosity, Sw= Water saturation, Bo = Oil formation Volume Factor.

#### 4.4. Volumetric Analysis

The volumetric estimate of each reservoir was computed using the depth structure maps and petrophysical parameters such as reservoir thickness, porosity, net-to-gross reservoir (NTG) and water saturation, obtained from the well logs (Figure 8A – Figure 8E). The formation volume factor was obtained from analogue fields due to the absence of pressure–volume–temperature (PVT) data or reports for the Baze field. Equation 6 and 7 was adopted for the calculation of the volumetric estimate of Baze Field.

The results of the volumetric estimates are presented in Table 9 and Table 10. Based on the volumetric approach described above, the stock tank oil initially in place (STOIIP) was estimated to be 40.384 MMbbls as shown in Table 9. With a recovery of about 30 %, only about 12.115 MMbbls can be produced from the reservoirs. The porosity of the reservoirs ranges from 0.23-0.28. According to the porosity description by [13], the quantitative description of the reservoirs can be characterized as very good. Similarly, the gas initially in place (GIIP) was calculated to be 14.094 Bscf and with a recovery of about 60 %, only 8.456 Bscf can be produced from the reservoirs.

#### 5. Conclusion

3-D Seismic and well log data have been used to characterize the Hydrocarbon-bearing sand bodies within the subsurface in the Baze field, Onshore Niger Delta. Time and depth structural maps of five horizons were generated. These maps revealed the structural geometry of the subsurface and the trapping mechanism which controlled the hydrocarbon accumulations in the field. The faults interpreted describe the structural setting of the field which showed two major faults and some synthetic and antithetic faults. The trend of the two major growth faults was in the East–West direction (E–W), both dipping in the South direction. These major faults were used to define the regionally extensive structures with rollover anticlines that were formed as a result of deformation of the sediments deposited on the downthrown fault block.

It can be inferred from the above that the results from this research work signify that a recoverable amount of oil and gas could be determined from the field of study depicting how economically significant the onshore Baze field in the Niger Delta was during the time of this study.

#### Acknowledgements

The authors appreciate Oriental Energy Resources Limited for providing all the data that were used in this research work. The authors are grateful to Baze University.

#### References

- [1] Whiteman A. J., 1982. Nigeria: Its petroleum geology, resources and potential. First ed. Springer, Netherlands.
- [2] Doust H., 1990. Petroleum geology of the Niger delta. J. Brooks ed., Classical petroleum provinces: Geological Society (London), Special Publications 50, 365-365.
- [3] Short K. C. and Stauble A. J., 1967. Outline of geology of Niger Delta. AAPG bulletin 51, 761-779.
- [4] Sheriff R. E., and Geldart L. P., 1995. Exploration Seismology. Second ed. Cambridge University press, UK.
- [5] Daukoru J. W., 1975. PD 4(1) Petroleum geology of the Niger Delta. World Petroleum Congress, 11-16 May, Tokyo, Japan.
- [6] Lehner P., and Ruitter P. D., 1977. Structural history of Atlantic margin of Africa: AAPG Bulletin, 61, 961-981.
- [7] Kulke H., 1994. Regional petroleum geology of the world, Part I: Europe and Asia. Gebrüder Borntraeger-Berlin-Stuttgart.
- [8] Evamy B. D., Haremboure J., Kamerling P., Knaap W. A., Molloy F. A., and Rowlands P. H. 1978. Hydrocarbon habitat of tertiary Niger Delta: AAPG bulletin, 62, 1-39.
- [9] Allen J. R. L., 1965. Late Quaternary Niger Delta, and adjacent areas: sedimentary environments and lithofacies. AAPG Bulletin, 49, 547-600.
- [10] Tuttle M. P., Collier J., Wolf L. W., and Lafferty R. H., 1999. New evidence for a large earthquake in the New Madrid seismic zone between AD 1400 and 1670. Geology 27, 771-774.
- [11] Larionov V. V., 1969. Borehole Radiometry, Nedra, Moscow.
- [12] Asquith G., Krygowski D., Henderson S., and Hurley N. 2004. Basic well log analysis: AAPG methods in exploration series 16. American Association of Petroleum Geologists, Tulsa, Oklahoma, USA.
- [13] Rider M. H., 1986. The geological interpretation of well logs. Second ed. Blackie, London.